Anal. Chem. **2002,** *74,* 386−393

Single-Molecule Resolution and Fluorescence Imaging of Mixed-Mode Sorption of a Dye at the Interface of C_{18} and Acetonitrile/Water

Melody D. Ludes and Mary J. Wirth*

Department of Chemistry & Biochemistry, University of Delaware, Newark, Delaware 19716

Single-molecule imaging is used for the first time to study the cationic dye, 1,1′-dioctadecyl-3,3,3′3′-tetramethylindocarbocyanine perchlorate (DiI), at the chromatographic interface consisting of acetonitrile/water and a hydrocarbon monolayer (C_{18}) covalently bound to silica. Autocorrelations of burst data agree with our previous single-molecule counting results, showing that most dye molecules are diffusing and that there is a rare specific adsorption site associated with a 0.07-s desorption time. These autocorrelations go further in detecting an even rarer specific adsorption event associated with a 2.6-s desorption time. The latter desorption time would contribute much more significantly to peak tailing in chromatography. In water, the populations of DiI at these two specific adsorption sites are shown to be 11% and 4%, respectively, for the weaker and stronger sites, relative to the diffusing population of DiI. In 60% acetonitrile/water, the relative populations of the specific adsorption sites are 11% and 17%, showing that acetonitrile enhances the population of the stronger specific adsorption site. Fluorescence movies of single and multiple molecules link the stronger specific adsorption sites to specific locations on the surface. The imaging makes rare observations frequent by pinpointing where the events occur spatially. This ability to observe rare events by imaging reveals the presence of a third type of specific adsorption site, for which DiI has a desorption time in excess of 20 s.

The strong specific adsorption of organic bases to silica surfaces in reversed-phase chromatography causes peak tailing and poor resolution.[1−4] Tailing is believed to be caused by mixed-mode retention, where there are two disparate types of adsorption sites: the intended organic monolayer and the residual silanols.[5] The analyte interacts weakly with the abundant organic monolayer and strongly with the rare exposed silica sites. Numerous experiments have been performed to understand interactions between organic bases and these silanols, as presented in review articles by Nawrocki[6] and Cox.[7] Many ways exist to reduce the number or effect of silanols on the surface and, hence, the tailing of chromatographic peaks. These include end capping[8] or other ways of achieving full coverage of the silica,[9] using mobile-phase additives,[10−13] lowering the pH of the mobile phase,[14,15] and removing metal impurities from the silica.[16,17] While useful for reducing tailing, these techniques do not entirely eliminate tailing, and its mechanism is not fully understood.

Studies of the sorption kinetics of organic cations to chromatographic interfaces aid in the understanding of how silica sites affect tailing. Several different types of experiments have been devised to probe sorption kinetics. Pyda et al. applied the expectation−maximization method to GC data to determine the adsorption energy distributions of several molecular probes on two bare silica gel samples.[18] From their results, they concluded that the surfaces of the silica samples are heterogeneous. For example, methanol has a bimodel distribution of adsorption energy. They also modified the silica samples with trimethylchlorosilane and found a decreased total magnitude of adsorption but a relative increase of the importance of the higher energy adsorption sites. Köhler et al. combined FT-IR with chromatography to show that the abundance of isolated silanols is correlated with the amount of tailing for basic compounds eluted from silica-based materials.[19,20] Wirth et al. showed evidence from fluorescence imaging of a dye that the specific adsorption sites on fused

(1) McCalley, D. V. *J. Chromatogr., A* **1997**, *769*, 169−178.
(2) Neue, U. D.; Phillips, D. J.; Walter, T. H.; Caparella, M.; Alden, B.; Fisk, R. P. *LC/GC* **1994**, *12*, 468−473.
(3) Fornstedt, T.; Zhong, G. M.; Guiochon, G. *J. Chromatogr., A* **1996**, *741*, 1−12.
(4) Gotmar, G.; Fornstedt, T.; Guiochon, G. *J. Chromatogr., A* **1999**, *831*, 17−35.
(5) Lenhoff, A. M. *J. Chromatogr.* **1987**, *384*, 285−299.
(6) Nawrocki, J. *J. Chromatogr., A* **1997**, *779*, 29−71.
(7) Cox, G. B. *J. Chromatogr., A* **1993**, *656*, 353−367.
(8) Yamaguchi, J.; Hanai, T. *J. Chromatogr. Sci.* **1989**, *27*, 710−715.
(9) Fairbank, R. W. P.; Xiang, Y.; Wirth, M. J. *Anal. Chem.* **1995**, *67*, 3879−3885.
(10) Yang, H.; Thyrion, F. C. *J. Liq. Chromatogr. Relat. Technol.* **1998**, *21*, 1347−1357.
(11) Gill, R.; Alexander, S. P.; Moffat, A. C. *J. Chromatogr.* **1982**, *247*, 39−45.
(12) Park, J. H.; Ryu, Y. K.; Lim, H. J.; Lee, H. S., Park, J. K.; Lee, Y. K.; Jang, M. D.; Suh, J. K., Carr, P. W. *Chromatographia* **1999**, *49*, 635−642.
(13) McCrossen, S. D.; Simpson, C. F. *J. Chromatogr., A* **1995**, *697*, 53−58.
(14) Dolan, J. W.; Snyder, L. R.; Saunder, D. L.; Van Heukelem, L. *J. Chromatogr., A* **1998**, *803*, 33−50.
(15) Roses, M.; Oumada, F. Z.; Bosch, E. *J. Chromatogr., A* **2001**, *910*, 187−194.
(16) Kimata, K.; Tanaka, N.; Araki, T. *J. Chromatogr.* **1992**, *594*, 87−96.
(17) Nawrocki, J.; Moir, D. L.; Szczepaniak, W. *Chromatographia* **1989**, *28*, 143−147.
(18) Pyda, M.; Stanley, B. J.; Minngao, X.; Guiochon, G. *Langmuir* **1994**, *10*, 1573−1579.
(19) Köhler, J.; Chase, D. B.; Farlee, R. D.; Vega, A. J.; Kirkland, J. J. *J. Chromatogr.* **1986**, *352*, 275.
(20) Köhler, J.; Kirkland, J. J. *J. Chromatogr.* **1987**, *385*, 125−150.

10.1021/ac010943u CCC: $22.00
Published on Web 12/11/2001

silica are preferentially located at nanometer-deep polishing marks, introducing substrate topography as a factor in tailing.[21] The polishing pattern disappeared with end capping, indicating that substrate topography sterically hinders the coverage of C_{18}. Rivera et al. studied the adsorption of ethyl acetate and 2-propanol from *n*-heptane solution onto bare silica sol−gel thin films, using attenuated total internal reflection FT-IR.[22] Their experiments detected both the adsorbate and the change in infrared spectrum of the functional group on the silica surface. The results revealed two types of adsorption sites on the silica surface for ethyl acetate. By examining the OH stretching and water bending regions of the spectra, they concluded that the two adsorption sites are isolated silanols and surface water adsorbed on vicinal silanols, with the former being 1 order of magnitude stronger. Wirth and Swinton used single-molecule spectroscopy to count diffusing and specifically adsorbed molecules at the interface of water and C_{18} on silica, and their results showed abundant weak adsorption sites and one type of rare specific adsorption site, with the latter having a desorption time on the order of 100 ms.[23] This short of a desorption time would typically cause more broadening than tailing. It is possible that stronger, rarer specific adsorption sites exist on fused silica but were not observed due to the low number of events in counting single molecules.

A larger number of adsorption events can be studied by fluorescence correlation spectroscopy, which employs autocorrelation of single-molecule bursts. It has recently been shown that autocorrelation of single-molecule bursts reveals quantitative information about adsorption equilibria: the relative concentrations of adsorbing and diffusing species, $\Gamma_{ads}/\Gamma_{diff}$, the rate constant for desorption, $1/\tau$, and the diffusion coefficient, D, of the fluorescing species.[24] If there are multiple specific adsorption sites, i, the contributions are additive, as shown in eq 1.

$$G(T) = \frac{\epsilon_{diff}\gamma_{diff}}{1 + D\frac{T}{s^2}} + \epsilon_{ads}\gamma_{ads}\sum_i \frac{\Gamma_{ads,i}}{\Gamma_{diff}} \exp(-T/\tau_i) \qquad (1)$$

The molar adsorptivities and quantum efficiencies, ϵ and γ, could differ for the adsorbed (ads) and diffusing (diff) species. It was shown that the beam variance, s^2, affects how easy it is to observe the exponential contribution from specific adsorption.[24]

The purpose of this work is to employ the increased observation rate of fluorescence correlation spectroscopy to investigate the number of different types of specific adsorption sites on silica under reversed-phase conditions. We also use fluorescence imaging with single-molecule spectroscopy to study the spatial heterogeneity of specific adsorption. The fluorescent dye, 1,1′-dioctadecyl-3,3,3′,3′-tetramethylindocarbocyanine perchlorate (DiI), at the solvent/C_{18}−SiO_2 interface, is studied for water and for 60% acetonitrile/water.

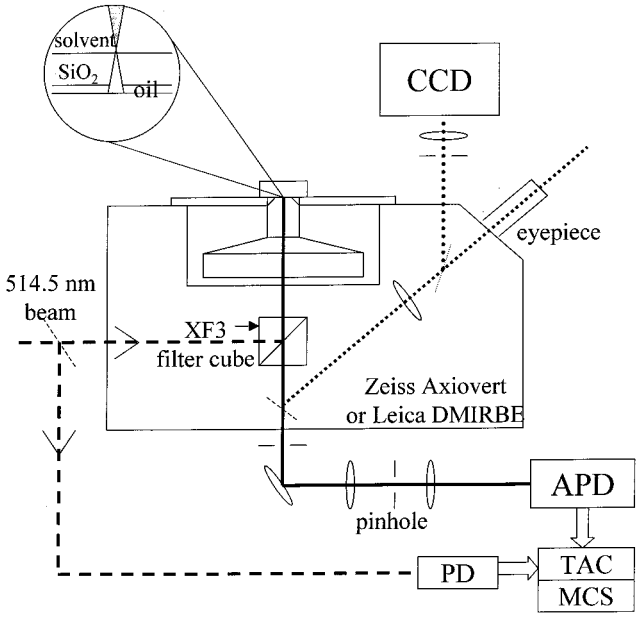

Figure 1. Schematic diagram for all experiments performed here. The single-molecule burst data were acquired using the Zeiss Axiovert, the external confocal pinhole, and time filtering with the time-to-amplitude converter (TAC) to reject Raman emission. The data were acquired by the multichannel scalar (MCS). The imaging experiments used the Leica DMIRBE and an intensified CCD camera.

EXPERIMENTAL SECTION

Sample Preparation. Fused-silica coverslips were obtained from ESCO Products, Inc. (R425025, 25 mm × 25 mm × 170 μm). These were cleaned in a 50:50 mixture of nitric acid and then rinsed with water, which had been purified to a resistance of 18 MΩ·cm using a Barnstead E-pure system. Next the coverslips were chemically modified with chlorodimethyloctadecylsilane (United Chemical Technologies) by refluxing in dry heptane, with *n*-butylamine as a catalyst. The heptane and *n*-butylamine were obtained from Fisher Scientific and Sigma, respectively. A surface coverage of 3.3 μmol/m^2 C_{18} groups is achieved via this method. The chemically modified coverslip was mounted in a Teflon flow cell and secured to the platform of an inverted microscope. To achieve a suitable dye concentration for imaging, DiI was deposited on the surface by first exposing the surface to 1 mL of a 20 nM stock solution of the dye in acetonitrile and then rinsing several times with acetonitrile until the concentration is reduced enough to allow observation of individual molecules diffusing through the excitation beam. The acetonitrile is replaced with the solvent or solution of interest. The acetonitrile was HPLC grade obtained from Aldrich.

Single-Molecule Spectroscopy. The instrumental setup used in the single-molecule experiment is similar to the one used previously[23] and is shown in Figure 1. The 514.5-nm line of a mode-locked argon ion laser was directed into the back port of a Zeiss Axiovert 100 inverted microscope, which had a filter set optimized for detection of DiI (Omega Optical, XF32). Raman emission from the solvent was reduced by adding a cutoff filter (610-nm EFSP) to the filter set. A 100× oil immersion objective with a numerical aperture of 1.40 was used to both focus the laser beam on the surface and collect the fluorescence. Approximately 3 μW of power was focused to a beam variance (0.85 μm)^2. The small beam variance causes the contribution from diffusion to decay very

(21) Wirth, M. J.; Ludes, M. D.; Swinton, D. J. *Anal. Chem.* **1999**, *71*, 3911−3917.
(22) Rivera, D.; Poston, P. E.; Uibel, R. H.; Harris, J. M. *Anal. Chem.* **2000**, *72*, 1543−1554.
(23) Wirth, M. J.; Swinton, D. J. *Anal. Chem.* **1998**, *70*, 5264−5271.
(24) Wirth, M. J.; Ludes, M. D.; Swinton, D. J. *Appl. Spectrosc.* **2001**, *6*, 663−669.

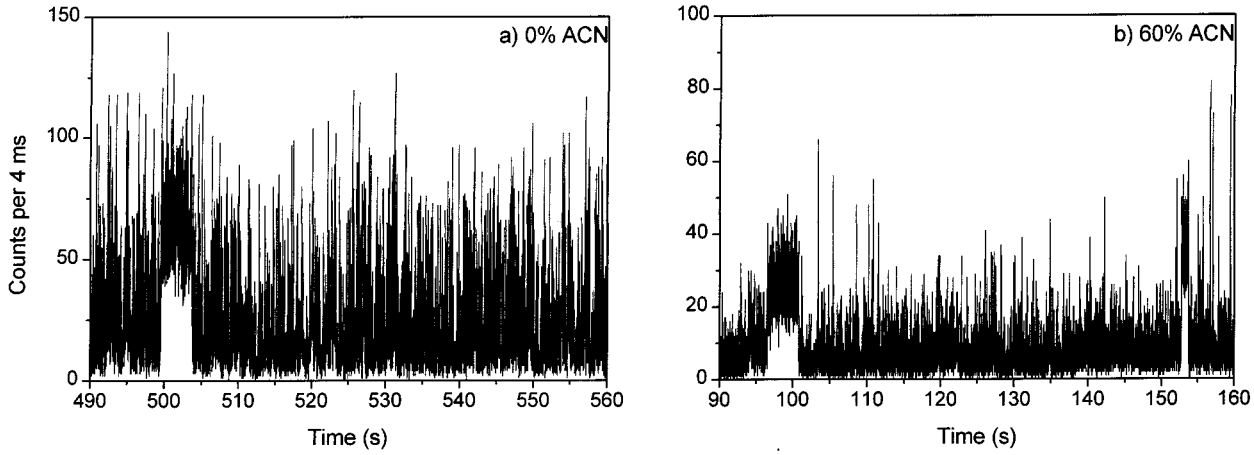

Figure 2. Single-molecule burst data for solvents (a) water and (b) 60% acetonitrile/water. These are selected regions from a large data set chosen to illustrate the presence of specific adsorption events persisting on the time scale of seconds.

rapidly, making it easier to discern desorption events in the autocorrelation.[24] Further reduction of the background signal was accomplished using spatial filtering with a confocal pinhole. The fluorescence was imaged onto the active area of an avalanche photodiode, which was placed in the final image plane. Additional reduction of background from Raman emission was achieved by time filtering using a time-to-amplitude converter (Tennelec 863), where the stop pulse was provided by the sync out from the mode locker and the start pulse from the avalanche photodiode. The output was sent to a multichannel scalar, with the dwell time set to 4 ms, to give an acquisition time of 65.5 s for the 16 384 bins for each scan, and 10 scans were made for each experiment.

Fluorescence Imaging. The instrumental setup for the imaging experiments is also shown in Figure 1. The 514.5-nm line of an air-cooled argon ion laser was used for fluorescence excitation, with a grating to disperse the laser lines. The beam was focused to a diameter of 20 μm at the interface in order to obtain the fluorescence images, and the average power was maintained below 10 μW to avoid photobleaching. A Leica DM-IRB inverted microscope with TRITC filters (Omega Optical) was used with a 100× oil immersion objective for focusing the laser at the interface and for collecting and imaging the fluorescence onto the focal plane of a CCD camera. A Roper Scientific ICCD camera (I-Pentamax-512-EFT GIII) was used with thermoelectric cooling. An integration time of 1 s/frame was used, and 300 frames were acquired sequentially with a data-transfer time between frames of 0.022 s. The images were analyzed by exporting the data as text files, which were read and analyzed by programs written in Matlab, and the data were plotted using Microcal Origin. These programs include summing the frames to obtain cumulative images, plotting intensity versus time for selected pixels, and autocorrelating intensity versus time for selected pixels. The data from the cumulative images were exported to MathCAD for contour plots, which were captured by JASC Paintshop Pro for display.

RESULTS AND DISCUSSION

Burst data were acquired using dye concentrations ~10-fold higher than our previous study, where there was one molecule in the beam 13% of the time.[23] Figure 2 shows raw burst data for the two different solvents, 0% and 60% acetonitrile, where the same concentration of dye was used in both cases. Solvent could be changed without loss of dye because the dye is insoluble in both solvents. The time intervals displayed in Figure 2 were chosen because a very long adsorption event occurred in each case. For 0% acetonitrile, in Figure 2a, the burst beginning at 499 s lasts for 5 s. For 60% acetonitrile, in Figure 2b, a similarly long event is shown, beginning at 96 s. A second long event is evident at 154 s. These data are representative of the fact that specific adsorption events having durations longer than 1 s occurred and that these occur more frequently for 60% than for 0% acetonitrile. In our previous experiments, where we used water as the solvent, we saw no adsorption events longer than 1 s. Here, for the same acquisition time, but with 10-fold more molecules in the beam, we now observe a handful of obvious specific adsorption events longer than 1 s for water and many more for 60% acetonitrile. While the higher concentration of DiI makes the phenomenon more prominent, the congestion from diffusing molecules makes it more difficult to count single adsorbed molecules reliably. Despite the congestion, the concentration is still sufficiently low to use the technique of fluorescence correlation spectroscopy, where the autocorrelation of the burst data can be used to extract quantitative information about the specific adsorption events.

Figure 3 shows the autocorrelations of burst data for the two different solvents, water and 60% acetonitrile. Both sets of autocorrelation decays fit well to eq 1, and the fitting parameters are summarized in Table 1. It is assumed that $\epsilon_i\gamma_j$ is the same for DiI in every site, for a given solvent. If this assumption does not hold, the relative populations of the different adsorption sites for a given solvent would be in error. Mei et al. showed that the spectra of single rhodamine B molecules in sol−gel films shift only a few nanometers upon change from solvated to dry states,[25] so our assumption of constant $\epsilon\gamma$ for a given solvent is unlikely to affect the interpretation, The results in Table 1 show that the diffusion coefficient is much faster for 60% acetonitrile, in agreement with a previous study of the effect of solvent on lateral diffusion.[26] The results also report the presence of two specific adsorption sites. The decay constants of the sites do not change detectably with solvent, but the relative populations do. To

(25) Mei, E,; Bardo, A. M.; Collinson, M. M.; Higgins, D. A. *J. Phys. Chem. B* **2000**, *104*, 9973−9980.
(26) Swinton, D. J.; Wirth, M. J. *Anal. Chem.* **2000**, *72*, 3725−3730.

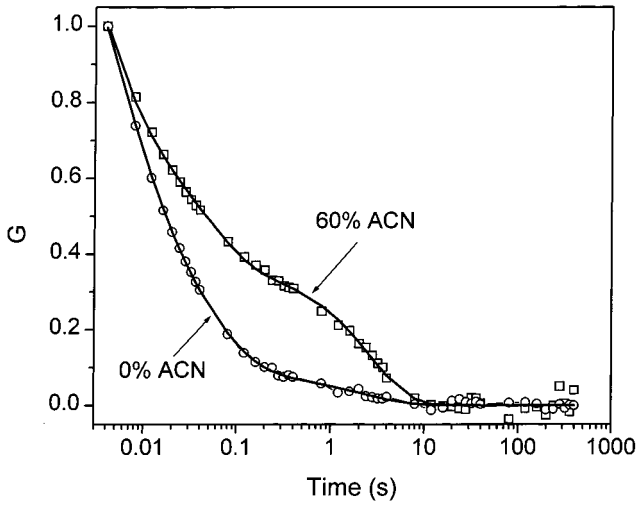

Figure 3. Normalized autocorrelation decays using the full data sets of bursts for water (○) and 60% acetonitrile/water (□). The solid curves are the best fit to eq 1 in each case, with the fitting parameters summarized in Table 1.

Table 1. Parameters Recovered from Best Fit to the Autocorrelations of Figure 6

	D (cm^2/s)	Γ_1/Γ_{diff}	τ_1 (s)	Γ_2/Γ_{diff}	τ_2 (s)
0% ACN	1.0×10^{-6}	0.11	0.068	0.04	2.6
60% ACN	6.5×10^{-6}	0.11	0.068	0.17	2.6

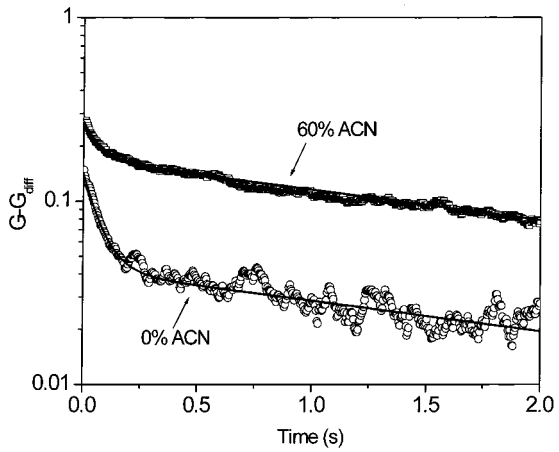

Figure 4. Same autocorrelation decays as in Figure 3, but with the contribution from diffusion subtracted out. The log G scale helps illustrate that there are two components of the decay and they are exponential.

demonstrate that these parameters are not pulled out of noise, Figure 4 shows plots of the same autocorrelation decays of Figure 3, but with the contribution from the diffusion term subtracted out. These decays are plotted on a log G scale to linearize exponential decays. The graphs in Figure 4 demonstrate pictorally that there is the same double-exponential decay for each of the two solvents but the relative amplitudes of the two exponentials differ. The smooth curves in Figure 4, which were made from the parameters of Table 1, are plotted for comparison and they fit well in both cases. The two discrete exponential components correspond to two types of specific adsorption sites. For the case of water, which we studied previously, the more abundant decay component has a desorption decay constant of 0.07 s, which is in agreement with our previous estimate of 0.1 s.[23] Since the present paper examines a much higher number of molecules, the results newly reveal the presence of a slower decay component having a decay constant of 2.6 s. For 60% acetonitrile, the weaker specific adsorption site has the same relative concentration and the same decay rate as for water. Therefore, the weaker specific adsorption site appears to be insensitive to mobile phase. The stronger specific adsorption site has the same decay constant but has a 3-fold larger population of DiI for 60% acetonitrile than for water. One concern in the interpretation is that the comparisons are limited by the statistics of small numbers. To address this, the experiments were each repeated three times, and in each case, the 60% acetonitrile showed more of the stronger specific adsorption events than did the water. It can thus be concluded that increased acetonitrile promotes adsorption to the stronger site. Since 60% acetonitrile is more typical of reversed-phase chromatographic conditions than is water, and since the stronger site would contribute much more to tailing than would the weaker site, these results are ultimately important for designing new chromatographic materials.

A more quantitative comparison between solvents might be obtained by combining single-molecule spectroscopy or fluorescence correlation spectroscopy with imaging because locally rough regions appear to be where specific adsorption occurs.[21] If this were true, focusing to a locally rough region would greatly increase the probability of observing specific adsorption events, providing better statistics. Figure 5 shows fluorescence images of a region of the solvent/C_{18}−SiO_2 interface, where the solvent in Figure 5a is water and in Figure 5b is 60% acetonitrile/water. These images are the averages of 300 frames, each acquired in 1 s of integration time using the intensified CCD camera. The region was chosen because a group of polishing pits was found, and the beam was focused among the group. The pits were not characterized by AFM, but this was previously studied for surfaces from the same supplier, showing numerous nanometer-deep pits.[27] The comparison of the two images in Figure 5 shows that the polishing pits have much more imaging contrast in the case of 60% acetonitrile. Seven features, a−g, are pointed out in the case of 60% acetonitrile, and these are much weaker, if visible at all, for water. A study of the intensity as a function of time is necessary to establish directly that specific adsorption occurs in the bright spots, as opposed to a locally higher surface area causing more brightness.

For the spots a−f in Figure 5, the intensities as a function of time are shown in Figure 6, using the same labels a−f. Also shown, for comparison, are intensities versus time for nearby pixels. In Figure 6a, which corresponds to a barely visible spot well inside the beam, there are large intensity spikes that saturate the 4095 range of the camera's A/D buffer. The nearby pixel has constant low intensity, and the intensity in the brighter pixel often drops to the level of the nearby pixel. This behavior indicates that the spikes in the brighter pixel are due to isolated specific adsorption events. Most of these events persist on the scale of a few seconds, except for one event, starting at 210 s, which lasts for 13 s. This panel establishes that specific adsorption, which is

(27) Cuppett, C. M.; Doneski, L. J.; Wirth, M. J. *Langmuir* **2000**, *16*, 7279−7284.

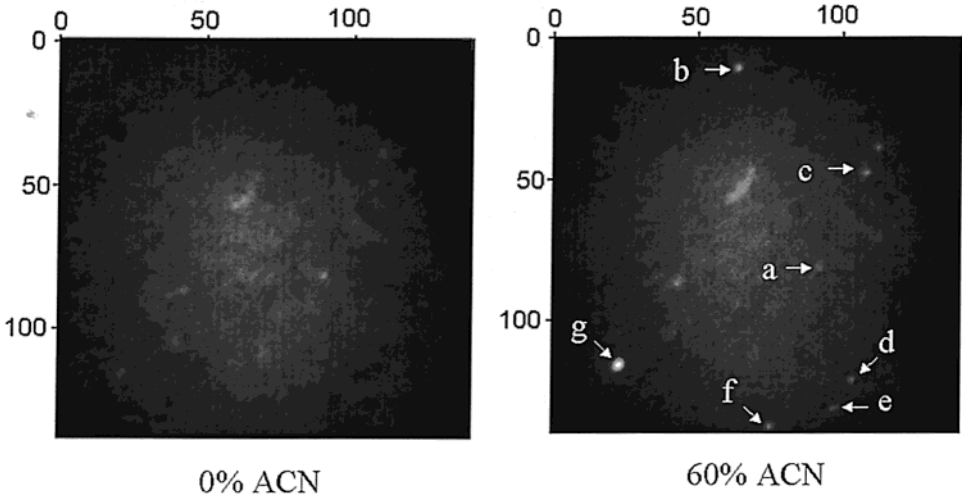

Figure 5. Fluorescence images of a region of a solvent/C_{18}−SiO_2 interface with many molecules of adsorbed DiI for the two solvents, (a) water and (b) 60% acetonitrile/water. The images were acquired by adding 300 sequential frames, where each frame was acquired in 1 s of integration time and 0.022 s of transfer time. The coordinate system is in units of pixels, with the entire 150-pixel range corresponding to 17 μm. For the specific features in the right panel, labeled a−f, the frame-to-frame intensities are plotted in Figure 6.

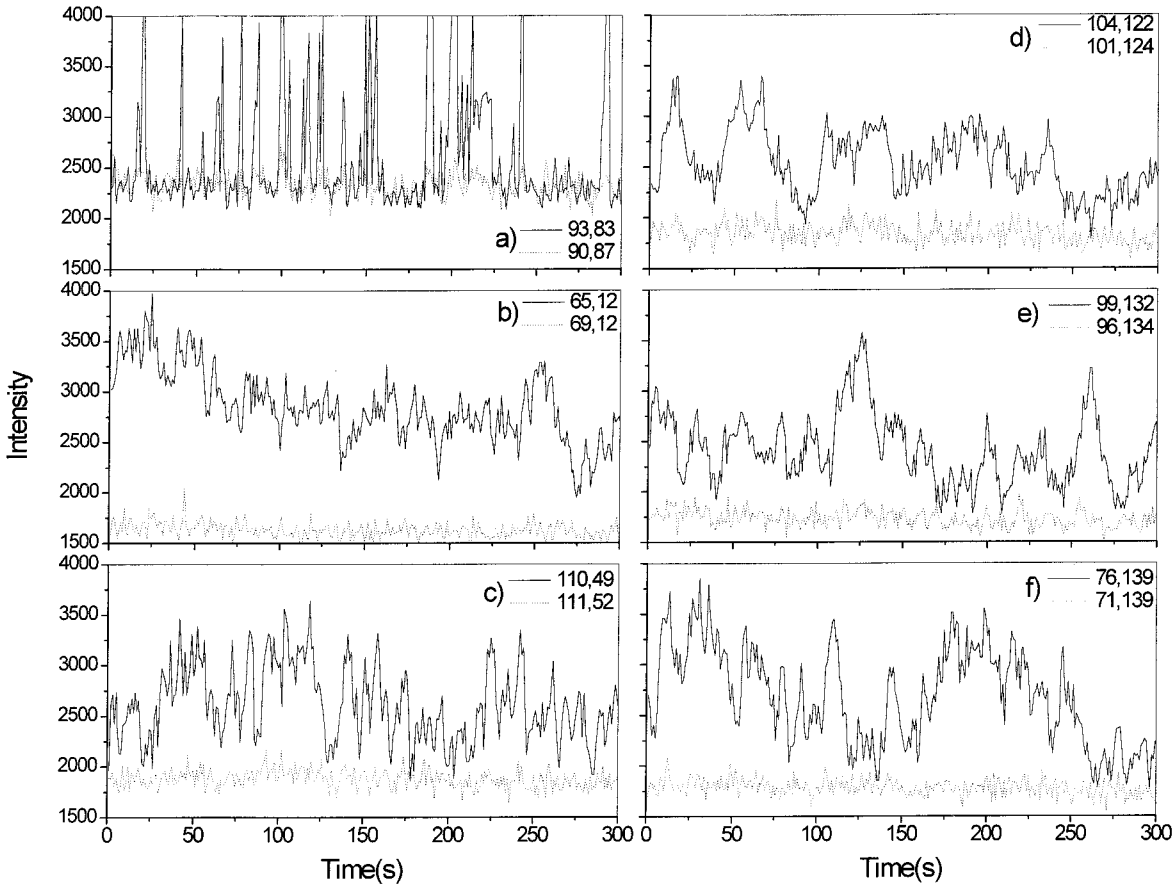

Figure 6. Intensity as a function of time for positions labeled a−f of Figure 5, where the solvent is 60% acetonitrile/water. The solid lines correspond to the positions labeled in Figure 5, and the dotted lines are for positions two pixels away. The coordinates in pixels are listed for each point.

rare over the entire interface, occurs frequently in a local region. The integration time of 1 s prevents any conclusion about the more abundant 0.07-s events, but the more important 2.6-s events are resolved. These events are expected to obey Poisson statistics. Figure 7A shows a histogram of the duration of desorption times, and a plot of an exponential decay having a 2.6-s decay constant, for comparison. The histogram agrees well with this exponential decay, confirming the Poisson behavior and the 2.6-s decay constant. An autocorrelation of the durations also gives a best fit of 2.6 s, further linking the spot a with the long specific adsorption events detected in the confocal microscopy results of Figure 4. The one event shown in the histogram of Figure 7A that lasts for 13 s could either be due to a stronger specific adsorption site or to the nonzero probability of observing such an event for the site

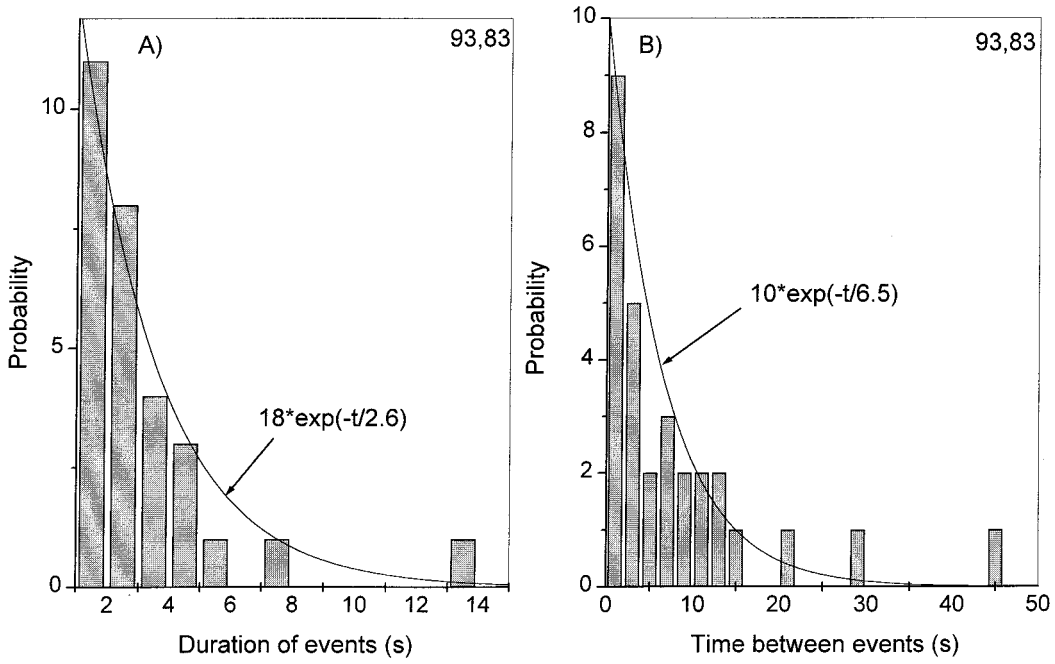

Figure 7. Poisson statistical plots from the intensity data in Figure 6a, corresponding to the point labeled a in Figure 5. (A) Histogram of the duration of adsorption events; (B) histogram of the time between adsorption events. The solid lines in each case are exponential decays with decay constants of (a) 2.6 and (b) 6.5 s.

having a 2.6-s decay constant. The probability of observing an event with a 13-s duration or longer, given the average desorption time of 2.6 s, is $P(13)$, which is 7×10^{-3}.

$$P(13) = \int_{13}^{\infty} \exp(-t/2.6)\, dt \qquad (2)$$

Given that 27 events were observed, the chances of one of them being as long as 13 s is $P(13) \times 27 = 0.18$, which means that the chance of observing such a long event is one in five. Nonetheless, it cannot be concluded without better statistics whether this event is due to a stronger site. It can be concluded that the spot a in Figure 5 stands out from the background because there is a locally high number of specific adsorption sites relative to the surrounding region. The adsorption events that give rise to this dim spot occur one dye molecule at a time. It can also be concluded that the average desorption time is in agreement with the 2.6-s desorption time observed in the confocal single-molecule fluorescence experiment.

The statistical behavior of the time between adsorption events should also behave in accord with Poisson statistics if adsorption occurs randomly. Figure 7B shows a histogram of the time between adsorption events and, for comparison, an exponential having a decay constant of 6.5 s. The behavior indicates that the adsorption process follows Poisson statistics. The Poisson behavior means that there is no bias toward readsorption once a molecule is desorbed. Thus, if the spot is a cluster of specific adsorption sites, they are sufficiently far apart that diffusion away from the spot occurs preferentially to readsorption, making the adsorption process random.

One would expect that the brighter the spot relative to its surroundings, the more frequent the specific adsorption events. Spots b−f are brighter, yet are further on the periphery of the beam; therefore, the adsorption events ought to be more frequent. Figure 6b−f confirms that this is the case. The fluorescence at these bright spots fluctuates due to these adsorption events but rarely drops to the background level of the nearby pixel. This figure shows that the intensity at each nearby pixel is constant over time. For spots b−f, the adsorption events are so frequent that there is significant overlap, indicating that there are numerous adsorption sites within the area of the pixel, which is large on the molecular scale, 180 nm^2. The exception that proves the rule is spot g, which is the brightest spot in the image of Figure 5. There is no fluctuation in intensity: the fluorescence remains at 4095 for every data point; hence, this point is not plotted. For spot g, the local density of adsorption sites must be sufficiently high that there is always at least one adsorbed molecule for each frame. Overall, these data directly tie specific adsorption events to bright features in the fluorescence image and show that there are clusters of specific adsorption sites within one pixel; i.e., the specific adsorption sites are not spatially resolved by the microscope.

The intensity fluctuations of Figure 6 can be autocorrelated to test whether they have the same 2.6-s decay constant as was found by the confocal microscopy. To maximize the signal-to-noise ratio, we averaged the autocorrelations for each spot, and the result is shown in Figure 8. We also autocorrelated the intensities for each of the nearby spots and averaged the autocorrelations, and the decay for these nearby spots is plotted in Figure 8, as well. There is significant amplitude only in the autocorrelation for the bright spots, not the nearby spots. The best fit is to a double-exponential decay, the first component of which is in excellent agreement with the 2.6-s decay constant. This confirms again that the 2.6-s decay component is associated with specific features on the surface. The autocorrelation of Figure 8 also shows that there is a second decay component that is on the order of 26 s in duration, and its population is approximately equal that that of the 2.6-s site. The

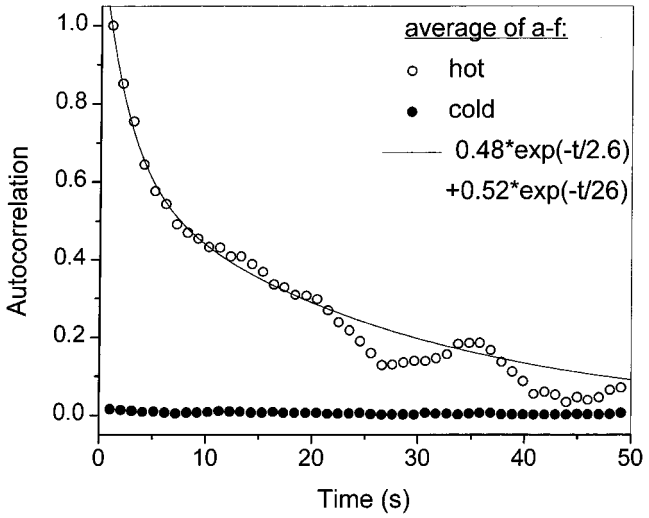

Figure 8. Comparison of autocorrelations for hot spots a−f in Figure 5 (○) and spots that are two pixels away (●). Each autocorrelation is the normalized sum of the individual autocorrelations of intensities in panels a−f of Figure 6.

ability to increase the observation rate of adsorption events by focusing in on local regions, where specific adsorption sites are clustered, enables this rarer event to be observed.

The longer the desorption time, the more relevant the site is to chromatography, provided it has a significant concentration of adsorbate. The strategy for observing relevant rare events can be formalized. The relative probability of observing a specific adsorption event to one site, *i*, compared to observing a specific adsorption event to another site, *j*, is calculated from the equilibrium dye concentrations, Γ, and desorption times, τ, for the two types of sites.

$$\frac{P_i}{P_j} = \frac{\Gamma_i/\tau_i}{\Gamma_j/\tau_j} \tag{3}$$

The longer the desorption time is, the greater the number of observations required, for the same concentration of adsorbed dye. In the case of DiI, since all three specific adsorption sites have comparable dye concentrations, and since their respective desorption times are 0.07, 2.6, and 26 s, there is about 1 order of magnitude lower probability of observation as these desorption times become progressively longer. The strongest adsorption site contributes negligibly in the confocal experiment, and this can be seen from the autocorrelations of Figure 3, which are noisy after 10 s, obscuring any information about events on the order of 20 s. The imaging experiment is more suited to studying these very long, very rare events because they occur much more frequently at these local spots. This underscores the need to tailor observation rate to the rarity of the phenomenon. Lengthy observation times could also be employed, but this is often impractical. We have recorded many single-molecule events for DiI at this same type of interface over the past few years, and we have made two observations of extremely long adsorption events. We observed a burst from a specific adsorption event persisting for 16 s on one occasion and a burst persisting for 55 s on another occasion, and these are shown in Figure 9. These establish by

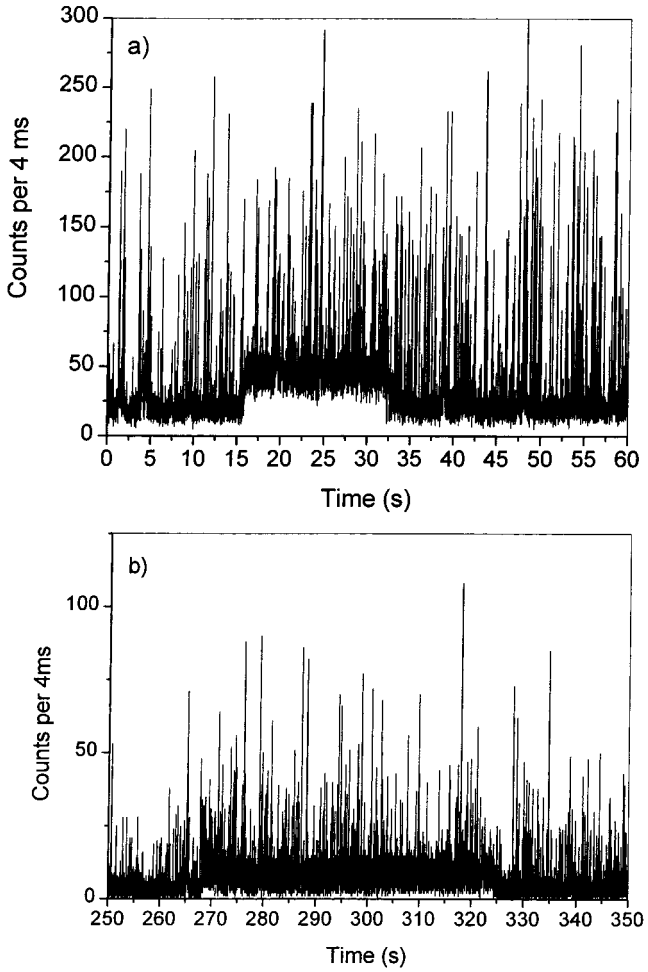

Figure 9. Single-molecule-burst data showing specific adsorption events persisting for (a) 16 and (b) 55 s.

direct single-molecule observation that ultralong adsorption events indeed occur. The new ability to take measurements at the position where strong adsorption occurs allows many more events to be observed. The rare ultrastrong events could be very important in chromatography because their low desorption rates would cause kinetic tailing under typical conditions.

Fused silica is amorphous, the topography of the polishing marks is uncontrolled, and the silica surface studied with the intensified CCD camera was a different sample from that studied by the confocal single-molecule microscopy, yet there is always the same discrete specific adsorption site having a 2.6-s decay time for DiI. This suggests that this site is fundamental to silica, rather than the way the silica was prepared. The surface heterogeneity that is evident in the fluorescence images shows that the abundance of the specific sites could be widely varied by preparation, particularly by varying how rough the surface is, but the chemical nature of the sites is apparently a property of silica. Consequently, this information might be pertinent to chromatographic silica gel. The probability of specific adsorption is thus an average property that varies locally with surface. Microscopically, the probability of specific adsorption could range from zero to unity. This could also be pertinent to chromatography because it is well known that different columns, even different lots from the same manufacturer, give different amounts of tailing.

One possible reason that specific adsorption would be more prevalent with 60% acetonitrile than with pure water is that the spots, which are located at polishing pits on the nanometer scale, would resist wetting by water. We added 5% propanol to the water, which is known to reduce the interfacial tension significantly, and over a time of a few seconds, the image of Figure 5a transformed to the image of Figure 5b. The solvent dependence of the specific adsorption appears to be a wetting effect.

The question that remains is the chemical identity of the specific adsorption sites. The various experiments that have been designed to investigate silanols all provide different pieces of information that are only beginning to come together. The most directly comparable experiment is the adsorption study by Rivera et al., where they showed that there are two types of adsorption sites on bare silica for ethyl acetate when *n*-heptane is the solvent.[22] They identified the weaker of the two adsorption sites as surface water and the stronger site as isolated silanols. The partition coefficients were shown to differ by 1 order of magnitude. It is possible that two of our three adsorption sites correspond to their adsorption sites and that the third site owes to the positive charge on DiI, whereas ethyl acetate is neutral. Another possibility is that there are multiple ways for DiI to adsorb. A third possibility is that there were too few of one of the sites to detect in their experiment, since the abundance of the specific adsorption sites varies with surface preparation. The experiments of Köhler et al.[19,20] detected chromatographic tailing, which is sensitive to desorption rates. They showed, by combining chromatographic measurements with FT-IR, that tailing correlates with the intensity of the isolated SiO−H stretch of isolated silanols. Tailing would become significant for desorption times slower than 1 s. This suggests that isolated silanols could be responsible for one or both of the specific adsorption events we observed having desorption times of 2.6 and 26 s. It is not known whether topographical features promote isolation of silanols. As more experiments are performed on silica surfaces, the gaps among these complementary experiments will be filled.

CONCLUSIONS

The surface of C_{18} on silica has at least four types of adsorption sites for DiI in 60% acetonitrile/water. The most prevalent site involves weak adsorption that allows the dye to laterally diffuse, and this is presumably the intended adsorption at the contiguous C_{18}/solvent interface. Three specific adsorption sites exist, with desorption times of 0.07, 2.6, and 26 s, and these sites have comparable dye concentrations of adsorbed dye at near-infinite dilution. The specific adsorption sites having desorption times of 2.6 and 26 s^{-1} are clustered at topographical pits on this sample of fused silica, where specific adsorption events are observable at a high rate locally. Acetonitrile enhances the population of DiI at these strong specific adsorption sites by wetting.

ACKNOWLEDGMENT

This work was supported by the National Science Foundation under gracnt CHE-0078847 and by Corning, Inc.

Received for review August 23, 2001. Accepted October 24, 2001.

AC010943U